

Microporous cationic nanofibrillar cellulose aerogel as promising adsorbent of acid dyes

Wafa Maatar · Sami Boufi

Received: 24 July 2016 / Accepted: 8 December 2016 / Published online: 23 December 2016
© Springer Science+Business Media Dordrecht 2016

Abstract Cellulose aerogel based on cationic cellulose nanofibrils (Q-CNF) with surface rich in trimethylammonium chloride functional groups was prepared by freeze drying and chemical crosslinking with an aliphatic triisocyanate. The aerogel, in the form of a rigid porous material, was shown to be an efficient adsorbent for anionic dyes and exhibited strong resistance to disintegration in water. The adsorption capacity for red, blue, and orange dyes was 250, 520, and 600 $\mu\text{mol g}^{-1}$ (about 160, 230, and 560 mg g^{-1}), respectively. Zeta potential measurements confirmed the main contribution of electrostatic interactions between positive sites on the CNF surface and dye sulfonate groups. The adsorption capacity was shown to be related to the specific surface area of the nanocellulose aerogel and the cationic content of the CNF. Spent Q-CNF adsorbent could be regenerated by extraction with KCl solution in ethanol–water mixture and reused for multiple adsorption–desorption cycles

without significant loss of adsorption capacity. Such Q-CNF aerogels show great promise for application as reusable adsorbents from a renewable resource for treatment of dye-loaded water.

Keywords Cellulose nanofibrils · Dye · Adsorption · Aerogel

Introduction

Nanocelluloses, specifically cellulose nanofibrils (CNFs), have attracted increasing attention, constituting one of the breakthroughs in nanostructured materials from renewable resources (Kalia et al. 2014; Abdul Khalil 2014). They show great promise for use in many applications, including nanocomposites based on nanocellulose (Boufi et al. 2014) and cellulose plastic films for use in packaging (Alcalá et al. 2013), food packaging, biomedical applications, as a strength additive for papers (González et al. 2012, 2013), drug delivery (García-González et al. 2011), implantable scaffolds (Mathew et al. 2012), and highly porous cellulose adsorbents (Maatar and Boufi 2015). Currently, cellulose nanocrystals (CNCs) and cellulose nanofibrils (CNFs) are the main families of nanocellulose produced by a top-down approach starting from cellulose fibers. They differ in their morphology and production method. CNCs are needle-shaped crystalline fibrils with length of

Electronic supplementary material The online version of this article (doi:10.1007/s10570-016-1162-0) contains supplementary material, which is available to authorized users.

W. Maatar · S. Boufi
Faculty of Science, University of Sfax-LMSE, BP 802,
3018 Sfax, Tunisia

S. Boufi (✉)
Faculty of Science, University of Sfax-LMSE, BP 1171,
3000 Sfax, Tunisia
e-mail: sami.boufi@fss.rnu.tn

150–300 nm and diameter of 5–10 nm, while CNFs are composed of nanosized, thin flexible fibrils, including both crystalline and amorphous domains with width of 5–50 nm and length on the micron scale. Although one of the most popular applications of CNFs is to reinforce a wide range of materials, including polymers, papers, cements, and hydrogels, the potential application of nanocellulose for environmental remediation and water treatment has recently drawn attention, more specifically as a new generation of nanostructured adsorbents obtained from renewable resources. Interest in use of CNFs as a new family of adsorbents for environment remediation is driven by several of their attributes, including: (1) high surface area (Dufresne 2013), which is beneficial for adsorption processes, (2) high aspect ratio favoring the establishment of an entangled (for CNF) network that contributes to enhanced mechanical cohesion of the adsorbent (Boufi 2014); (3) high stiffness and strength of CNF fibrils (modulus and strength in the ranges of 65–85, and 2–4 GPa, respectively; Tanpichai et al. 2012), helping to make the adsorbent more resistant and reusable without risk of disintegration; and (4) the varied possibilities for surface functionalization (Ey-ley and Thielemans 2014), which can extend the adsorption to a large class of chemical species.

However, the strong tendency of CNFs to self-aggregate via hydrogen bonding constitutes a main obstacle to their effective application for environmental remediation and water treatment. This irreversible aggregation results in a huge decline in the specific surface, inevitably resulting in a dramatic reduction in the adsorption capacity. Furthermore, aggregation hampers regeneration and reuse of such nanosized adsorbents in multiple cycles.

One approach to alleviate this shortcoming is processing CNFs in the form of a solid porous aerogel to preserve its structural integrity, offering the possibility of a continuous adsorption process. Such a three-dimensional interconnected porous structure supports the active adsorption sites within a solid network, preventing the tendency of CNFs to aggregation.

Successful production of such cellulose aerogels based on CNFs has been demonstrated in several publications, with freeze drying and supercritical CO₂ drying being the most efficient approaches to remove water or other solvent without risk of collapse due to the capillary effect. However, since the cohesion of

CNF aerogels is based on hydrogen bonding and physical entanglement, their structural stability is inevitably lost in contact with water, due to its diffusion inside the CNF network and destruction of cellulose–cellulose hydrogen bonds. Chemical crosslinking of cellulose aerogels via reactions involving hydroxyl groups was recently shown to be a successful alternative to improve their structural stability in aqueous media (Zhang et al. 2012); For example, chemical crosslinking of CNF aerogels through condensation of carboxylic groups of CNFs and azetidinium groups of Kymene was performed by Zhand et al. (2012). Another approach was recently reported by Kim et al. (2015), involving grafting of maleic acid onto CNFs, followed by reaction with hypophosphite.

Recently, the production and usefulness of cationic cellulose nanofibrils (Q-CNFs) have been the subject of several publications (Olszewska et al. 2011; Ho et al. 2011; Chaker and Boufi 2015; Saini et al. 2016). The potential of cationic Q-CNF as an adsorbent for organic dyes was demonstrated in the work of Pei et al. (2013), who used Q-CNF to prepare nanopapers with high mechanical properties and efficient dye adsorption. However, the adsorption mechanism and possible regeneration of the adsorbent were not explored. This new application of Q-CNFs opens the way to use of Q-CNFs as adsorbents for organic dyes.

The present work describes a novel route for production of Q-CNF aerogel covalently crosslinked with a triisocyanate and an investigation of its potential use as a reusable adsorbent for acid dyes.

Materials and methods

Materials

All chemical reagents provided by Aldrich were of analytical grade and used without further purification. Commercial bleached eucalyptus (*Eucalyptus globulus*) pulp was used as starting material for preparation of CNFs. Three textile dyes were used in the adsorption experiments: blue dye CR19, red dye 180, and orange dye 142, in their commercially available form. HDI-biuret was a commercial product from Bayer (Desmodur N100). Glycidyltrimethylammonium chloride (GMA) was a product from Aldrich.

Production of Q-CNFs

Q-CNFs were produced following the approach described in our previous work (Chaker and Boufi 2015). The method involves quaternization of bleached eucalyptus fibers by glycidyltrimethylammonium chloride, followed by disintegration via high-pressure homogenization to break up the cell wall and release CNFs.

Quaternization of cellulose fibers

Eucalyptus pulp was first soaked in distilled water for 12 h then subjected to mechanical disintegration using a domestic blender to obtain fiber suspension with 5 wt% concentration. The fiber suspension was then filtered to remove water and solvent-exchanged (twice) with dimethylacetamide (DMAC). Glycidyltrimethylammonium chloride (GMA, 1 g/g of dry fiber) was then added to the fiber suspension in DMAC (10 wt%) containing 0.2% KOH as catalyst and kept at 65 °C for 8 h. The reaction mixture was then centrifuged and washed five times with water to completely remove residual DMAC.

Fibrillation process

The fibrillation process was carried out by high-pressure homogenization using a GEA homogenizer processor (NS1001L PANDA 2K-GEA, Italy), in two steps. First, fiber suspension of quaternized fibers at concentration of 1.5 wt% was passed three times at pressure of 300 bar until the suspension turned into a gel. Fibrillation was then continued using five further passes at pressure of 600 bar. The resulting Q-CNF gel was transparent and viscous.

Q-CNF aerogel preparation and crosslinking

Q-CNF gel was packed in a glass cylindrical tube (h/D: 20/20 mm) and kept at −20 °C for 24 h to freeze the gel. The frozen sample was then transferred to a vacuum chamber at −50 °C and freeze dried at pressure of 0.05–0.02 mbar for 20–24 h until complete water sublimation. Crosslinking of the aerogel was carried out as follows: The dried aerogel pellet was soaked in solution of HDI-biuret isocyanate in toluene (0.5% by weight), and left at 60 °C for 6 h to

ensure reaction of the isocyanate function with hydroxyl groups of Q-CNF. The pellet was then removed and dried at 50 °C, and used as such.

Characterization of aerogel

The morphology of the Q-CNF aerogel was observed by scanning electron microscopy (SEM) using a JEOL JSM-6390LV operated at 5–10 kV. Prior to SEM analysis, the surface was coated with a gold/palladium layer. For higher-magnification observation of the cells of the aerogel, field-effect SEM was used on a thin sample deposited on a carbon tape followed by coating (sputtering) with a thin platinum layer.

Sample density was determined by weighing the aerogel and measuring its dimensions. The dimensions of each aerogel were measured at at least three different positions, and a minimum of two samples were used for density determination.

The porosity P of the aerogel is defined as $P = (1 - d_a/d_b) \times 100$, where d_a and d_b (1.56 g cm^{−3}) are the density of the aerogel and bulk cellulose fibrils, respectively.

Adsorption experiments

Weighed Q-CNF was soaked in a flask containing 50 ml dye solution, kept in a thermostated water bath shaker operated at 150 rpm at desired temperature for 3 h. In all experiments, the amount of dried gel sorbent was kept at around 200 mg. To obtain equilibrium data, the initial concentration of the dye solutions was varied while the amount of adsorbent was kept constant. All adsorption experiments were carried out at pH 7. The concentration of the dye remaining in aqueous solution was analyzed by visible spectrophotometry using an ultraviolet–visible (UV–Vis) spectrophotometer (PerkinElmer Lambda 35). For each sample, absorption spectra were recorded from 400 to 800 nm, and the absorption value at λ_{\max} was read for each time. The amount adsorbed q (mol/g) was calculated as

$$q_e = (C_0 - C_e) \cdot V/m, \quad (1)$$

where C_0 (mol/l) and C_e (mol/l) are the initial and final dye concentrations in solution, respectively, V (ml) is the volume of dye solution, and m (g) is the weight of aerogel.

Zeta potential measurements

Zeta potentials were measured at 25 °C using a laser Doppler electrophoresis apparatus (Malvern Nano-Zetasizer ZS, Malvern, UK). The sample concentration in water was set at 0.1% (w/v). Measurements were carried out in presence of Q-CNF gel without any crosslinking with isocyanate to preserve the electrophoretic mobility of the cellulose nanofibrils under the effect of the electrical field. Measurements were performed in triplicate for each sample, and average values are reported.

Regeneration of aerogel

Regeneration of the aerogel adsorbent was accomplished using KCl solution in a mixture of ethanol/water (50/50 vol%) as desorbing agent. The aerogels were soaked in 50 ml of solution and kept at temperature of 60 °C for 3 h. The desorption cycle was repeated twice, then the aerogel was washed with water several times and subjected to another adsorption cycle.

Continuous adsorption

Continuous adsorption experiments were carried out under isothermal conditions using a packed column filled with pellets of Q-CNF aerogel. The packed column employed was a jacketed glass column with diameter of 10 mm and length of 15 cm, packed with about 0.5 g aerogel pellets. Dye solution was percolated through the column from bottom to top using a precision peristaltic pump. Eluted samples were collected at regular intervals, and the concentrations monitored by UV–Vis spectrophotometer.

Antibacterial activity

The antibacterial activity of the films was tested against Gram-positive bacterium *Bacillus cereus* (ATCC 14579) and Gram-negative bacterium *Escherichia coli* (ATCC 25922), using the disc diffusion method on agar plate with slight modification.

The diffusion method was performed using Luria–Bertani (LB) medium solid agar in Petri dishes. The agar slurry on the test specimens was allowed to gel at room temperature, followed by incubation at 37 °C for 18 h. After incubation, films were cut into 15 × 15 mm² pieces,

sterilized in autoclave at 121 °C for 20 min, and kept in intimate contact with the bacterial agar gel. After incubation for 24 h at 37 °C, samples were examined visually for growth of bacteria in the area surrounding the film.

Results and discussion

Physical properties of solid aerogel

Crosslinked cationic aerogel was prepared in two steps. The first step was the production of Q-CNF by high-pressure homogenization of quaternized cellulose fibers with glycidyltrimethylammonium chloride according to a previously reported protocol (Chaker and Boufi 2015). Atomic force microscopy (AFM) images of Q-CNF confirmed the nanoscale dimension of the CNFs, revealing a network of entangled individual nanofibrils with typical width of around 5 nm and length in the micrometer range (Fig. 1). The size and surface charge characteristics of the Q-CNF are presented in Table 1.

Then, in the second step, samples of Q-CNF packed in a glass cylindrical tube were stored at –20 °C for 12 h and freeze dried to remove water. Sponge-like solid aerogel was obtained with shape similar to the frozen molded CNF gel. This Q-CNF aerogel was then cross-linked using a trifunctional isocyanate based on a biuret dimer of hexamethyldiisocyanate (HDI-biuret). After the crosslinking reaction and drying the aerogel, no change was observed neither on the shape nor on the density of the aerogel (Table 1). Scheme 1 depicts the different steps involved in preparation of the Q-CNF aerogel-based adsorbent.

The main objective of the treatment with HDI-biuret is to crosslink the CNF network to avoid the risk of physical disintegration during prolonged contact with water. This can be seen in Fig. 2, where the cross-linked aerogel sample shows no visible signs of disintegration after immersion in water for more than 12 h under magnetic stirring, while the non-cross-linked sample was totally broken up into fragments of aggregated fibrils after only 1 h of immersion in water. This supports the occurrence of covalent crosslinking of cellulose nanofibrils through chemical interaction with the trifunctional isocyanate. In fact, given the nanoscale size of the fibrils and the close proximity between them, forming an entangled network through hydrogen bonding, chemical crosslinking between

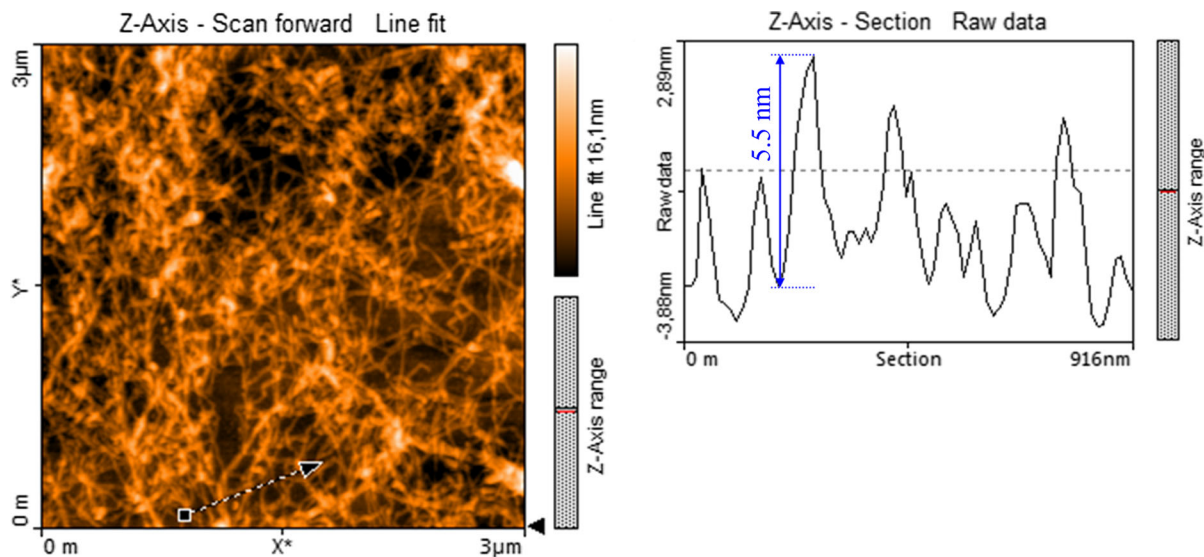


Fig. 1 AFM height images of Q-CNF and corresponding height profile analysis (the *arrow* marks the line used for height profile measurements)

Table 1 Physical characteristics of Q-CNF and Q-CNF aerogel after crosslinking with isocyanate

Characteristic	Q-CNF	Q-CNF aerogel
Width of nanofibrils ^a (nm)	5–7	
Fibrillation yield (%)	86	1084 ± 25
Trimethylammonium content ^b (μmol g ⁻¹)	1140 ± 25	
Zeta potential at pH 7 (mV)	+35	+37
Apparent density (g cm ⁻³)	–	0.0175 ± 0.0005
Porosity (%)	–	99 ± 5

^a AFM measurement (see supplementary data)

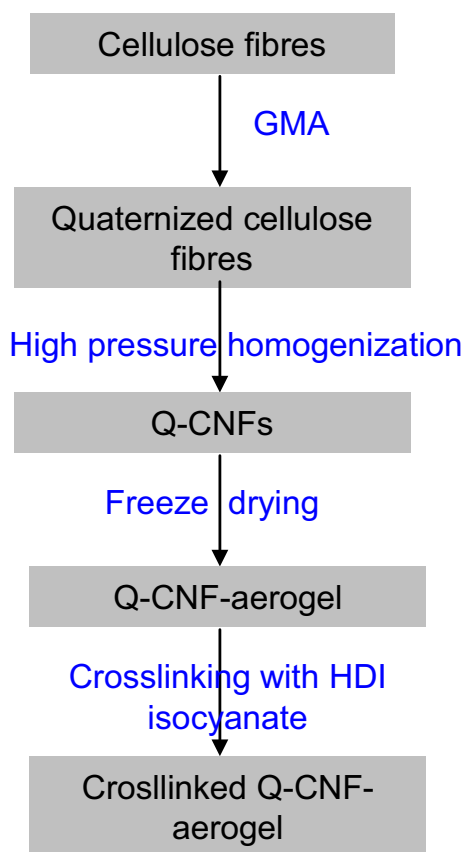
^b Conductometric titration of chloride ions with AgNO₃

neighboring nanofibrils can be envisaged. Indeed, if one considers the width of the cellulose nanofibrils to be about 5 nm and that hydrogen bonding requires close proximity (<0.35 nm) between neighboring hydroxyl groups, then the distance between two adjoining nanofibrils within the entangled network should be less than 0.5 nm. This distance is small enough to envisage chemical bridging between cellulose nanofibrils by reaction between the isocyanate function of HDI-biuret molecules (which have length of about 2.5 nm as estimated using ACD/3D software) and surface hydroxyl groups of crossing fibrils, as illustrated in Fig. 2.

Another positive effect of crosslinking with isocyanate is the improved flexibility of the aerogel. As seen in Fig. 3, the wetted aerogel totally recovered its original shape after compression, without any sign of

cracking or breaking. Both of these properties contribute to facilitate the reusability of the cellulose-based aerogel as a new class of nanostructured cellulose adsorbent for water treatment.

FE-SEM observation of a transversal cross-section of the aerogel (Fig. 4) revealed highly porous structure with cellular morphology formed by channels with width in the range of 20–50 μm. The cell wall of channels was quite thin with thickness in the range of 50–150 nm, which accounts for the low density and high porosity of the CNF aerogel. Magnification of the cell wall revealed random in-plane orientation of the nanosized fibrils with width on the order of 10–20 nm, forming a highly entangled network held through hydrogen bonding and chemical linking with the isocyanate.



Scheme 1 Steps to prepare Q-CNF adsorbent aerogel

Adsorption properties

The adsorption properties of the Q-CNF aerogel were investigated using three representative anionic dyes with differing chemical structure and number of sulfonate groups per molecule. The first evidence of the effectiveness of the Q-CNF aerogel as an adsorbent for acid dyes is the rapid change of color of the aerogel when placed in contact with aqueous dye solution. As shown in Fig. 5, when a piece (about 200 mg) of Q-CNF aerogel was immersed in 30 ml dye solution, the aerogel progressively colored, and total decoloration of the solution was observed after 45 min of contact time, with accumulation of the dye in the aerogel. No visible change in the shape or physical integrity of the aerogel was noted after adsorption.

The contact time required to reach equilibrium is a very important parameter for practical use of an adsorbent. The change in the amount of adsorbed dye with time was studied for the three dyes to assess the

adsorption kinetics. The results in Fig. 6 show that the adsorption process was quite fast for the tested dyes, with more than 80% of the adsorption capacity reached within 30 min. After this period, the adsorption rate decreased, and saturation was reached within about 60 min. Such efficient adsorption of the acid dyes by the Q-CNF aerogel is presumably due to the presence of trimethylammonium (TMA) groups on the surface of the CNFs, acting as binding sites for dye molecules bearing oppositely charged sulfonate groups.

Plots of q_e versus \sqrt{t} (Fig. 6) show that the adsorption kinetics could be fit using three linear segments. Such different linear portions indicate a multistep adsorption process with intraparticle diffusion playing a significant role in dye uptake by the Q-CNF aerogel (Ray 1996). The first linear portion is a boundary-layer effect associated with external transport of dye molecules from bulk solution to the outer surface of the adsorbent via molecular diffusion. The second portion is ascribed to intraparticle diffusion inside the internal pores of the aerogel. The third stage may be regarded as corresponding to diffusion through smaller pores, being followed by establishment of equilibrium.

To investigate the adsorption capacity and efficiency of the Q-CNF aerogel depending on the dye structure, adsorption isotherms were drawn for each dye (Fig. 7). The isotherms displayed a steep increase for concentrations below 0.2 mmol l^{-1} , followed by a mild increase until reaching a plateau corresponding to saturation of the adsorbent. The maximum adsorption capacity differed depending on the dye structure, reaching 293, 530, and $600 \text{ } \mu\text{mol/g}$ for the red, blue, and orange dye, respectively. The Q-CNF aerogel possessed high removal efficiency exceeding 95% for initial concentration below 0.1 mmol l^{-1} . Therefore, the developed Q-CNF-based aerogel is highly suitable for adsorption of anionic dyes.

The adsorption isotherms were fit using the Langmuir and Freundlich (Richard 1996) models, as expressed by Eqs. (2) and (3):

$$q_e = \frac{Q_{\max} \cdot k \cdot C_e}{1 + k \cdot C_e}, \quad (2)$$

$$q_e = K_f \cdot C_e^{1/n}, \quad (3)$$

where q_e and Q_{\max} (mol g^{-1}) are the adsorption capacity at equilibrium and the maximum adsorption capacity according to Langmuir monolayer

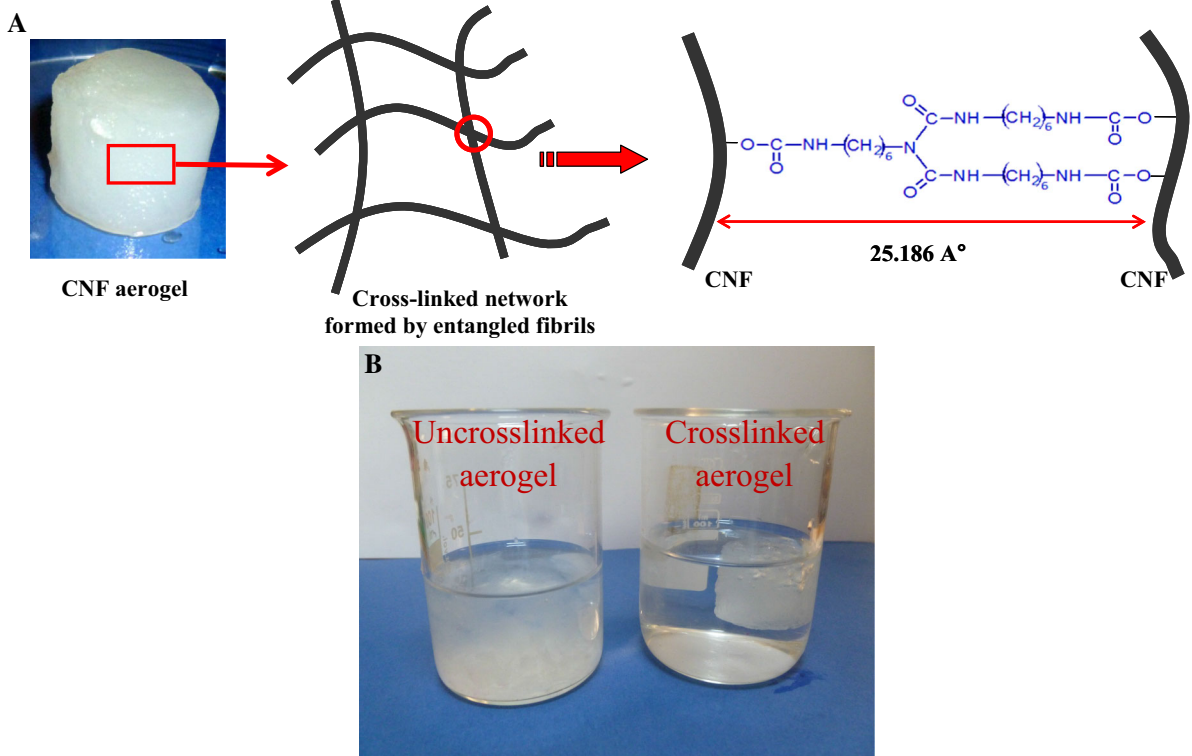
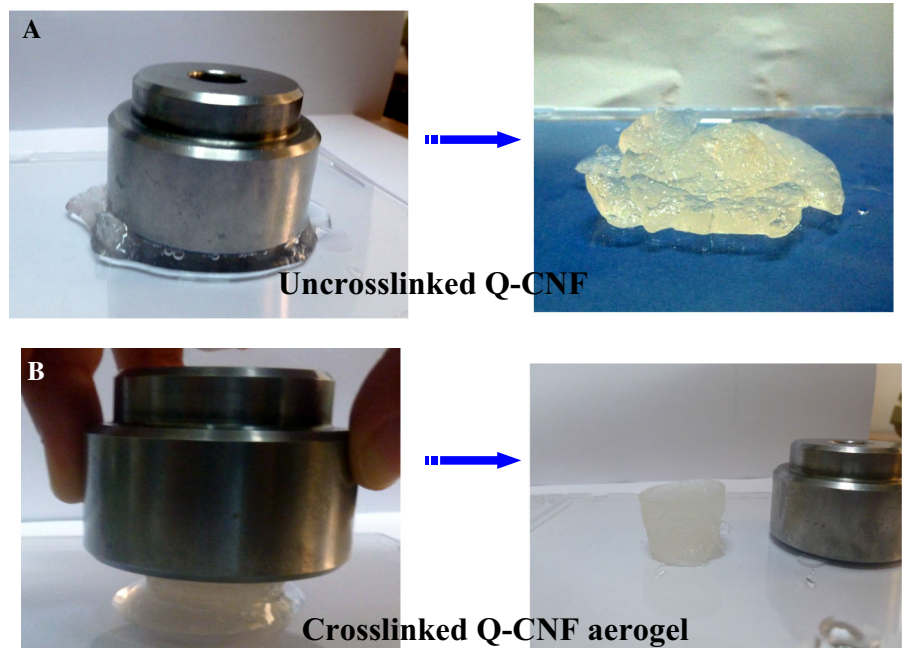


Fig. 2 **a** Chemical binding between adjacent CNFs (distance calculated using ACD/3D software), and **b** comparison of behavior of crosslinked and non-crosslinked Q-CNF aerogels in water

Fig. 3 Change in appearance after compression: **a** non-crosslinked, and **b** crosslinked aerogel



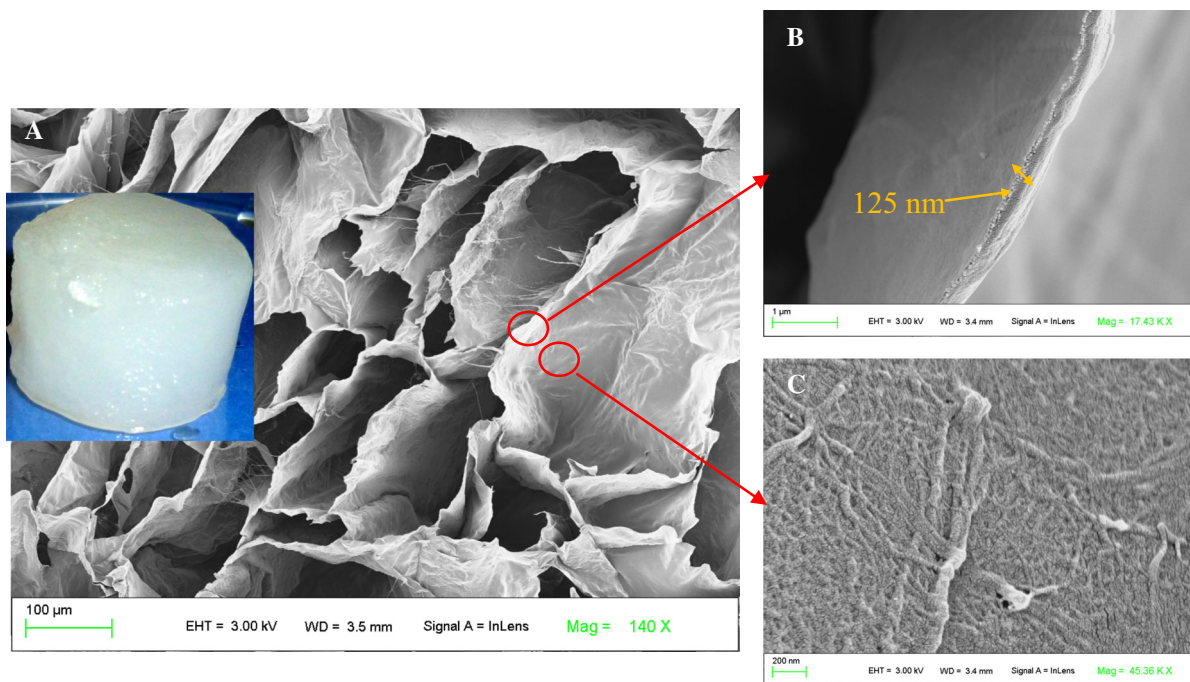


Fig. 4 FE-SEM images of **a** cryofractured surface of aerogel, with a magnification, **b** cross-section of cell wall of aerogel channel, and **c** structure of the wall, showing the network of entangled nanosized fibrils

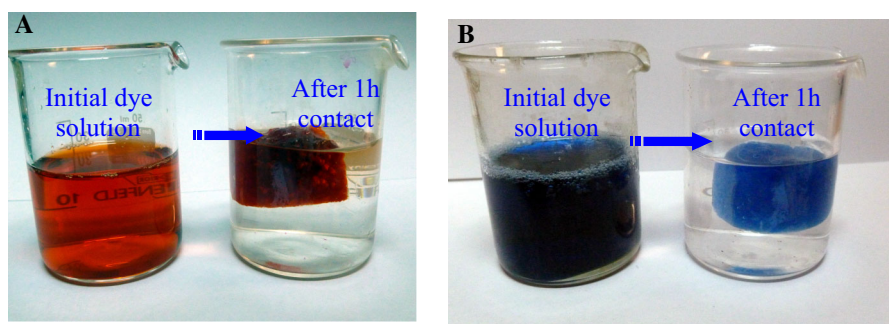


Fig. 5 Visual change in **a** orange and **b** blue dye solution after immersion of a Q-CNF aerogel tablet for 45 min (initial dye concentration = 10^{-4} M, volume = 30 ml, M_{Q-CNF} = 200 mg)

adsorption. C_e (mol l^{-1}) is the equilibrium concentration of dye, and k (l mol^{-1}) is the Langmuir constant, which is related to the free energy and affinity of the adsorbate for the binding sites. K_f (l mol^{-1}) and n are the Freundlich constants, related to the adsorption capacity and intensity of the adsorbent, respectively.

The Langmuir isotherm model is based on monolayer adsorption at a fixed number of well-defined, energetically equivalent sites, with no interactions between adsorbate species. The Freundlich isotherm

model is generally used to describe physical adsorption onto a heterogeneous surface and assumes that the adsorbed amount increases with the adsorbate concentration.

As seen from Table 2, the values of $1/n$ for both dyes were below 1, indicating favorable adsorption of the reactive dyes over the whole investigated concentration range (Yang and Al-Duri 2005). Based on linear plots of Eqs. (2) and (3), the parameters of the Langmuir and Freundlich isotherms were determined;

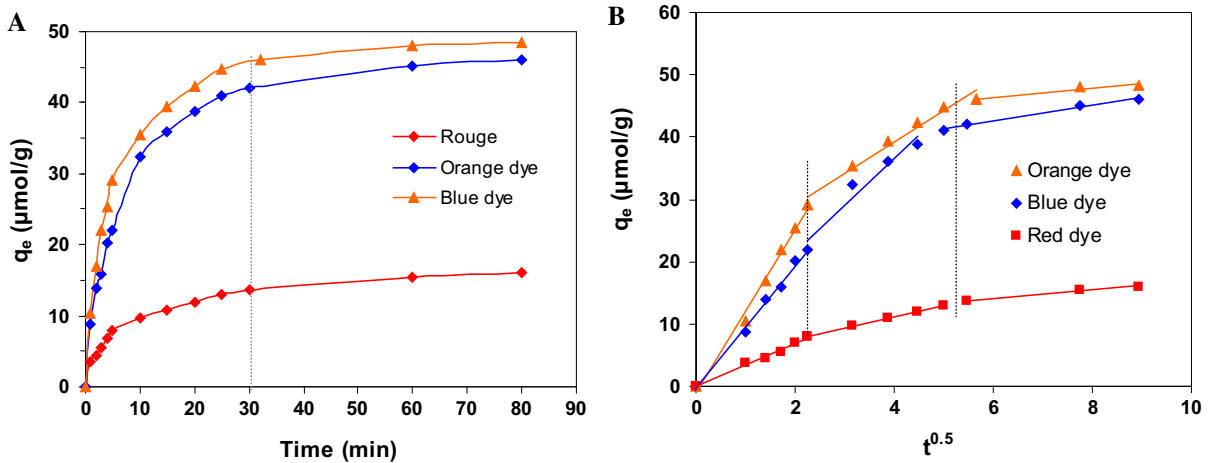


Fig. 6 a Kinetic adsorption of blue, orange, and red dyes, and b corresponding kinetic plots of q_e versus \sqrt{t}

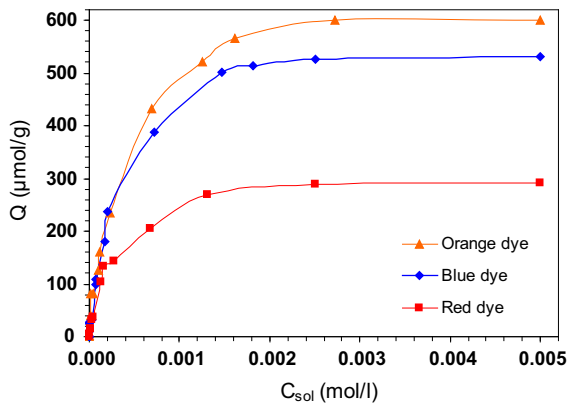


Fig. 7 Adsorption isotherms of dyes on crosslinked Q-CNF aerogel (conditions: pH 7, 200 mg Q-CNF, $T = 25\text{ }^\circ\text{C}$)

their values are given in Table 2. Based on the correlation coefficient, it can be seen that the Langmuir isotherm fit the experimental data better than the Freundlich model, in agreement with the adsorption being in the form of a molecular monolayer.

The dimensionless separation factor constant (R_L) was also estimated from Eq. (4):

$$R_L = \frac{1}{1 + K_L \cdot C_0} \tag{4}$$

According to literature, $R_L < 1$ denotes favorable adsorption, while $R_L = 0$ corresponds to irreversible adsorption (Hall et al. 1966). In this study, the R_L values were found to lie between 0.6 and 0.2 for initial

Table 2 Adsorption parameters according to Langmuir and Freundlich models

	Langmuir				
	Q_{\max} ($\mu\text{mol g}^{-1}$) ^a	Q_{\max} ($\mu\text{mol g}^{-1}$) ^b	K_L (l mol^{-1})	R_L	R^2
Blue dye 19	531	557	4556	0.418	0.98
Red dye 180	293	314	3314	0.448	0.998
Orange dye 142	600	627	4907	0.372	0.98
	Freundlich			R^2	
	$1/n$	K_F ($\mu\text{mol g}^{-1}$)			
Blue dye 19	0.506	10.957		0.917	
Red dye 180	0.607	3.273		0.914	
Orange dye 142	0.587	7.485		0.92	

^a Experimental value;
^b from Langmuir model

dye concentration between 10^{-4} and 10^{-3} M, implying favorable adsorption of the anionic dyes onto the Q-CNF aerogel.

Assuming monolayer adsorption of dye molecules with flat conformation, the total surface area (S) occupied by adsorbed dye molecules can be calculated as

$$S = S_{\text{dye}} \cdot NQ_{\text{max}}, \quad (5)$$

where S_{dye} is the surface area occupied by a single dye molecule, N is Avogadro's number (6.022×10^{23}), and Q_{max} is the maximum adsorption capacity in $\mu\text{mol g}^{-1}$. The dimensions and surface area of the dye molecules were determined using ACD/3D software (Table 3).

Using Eq. (5), the surface area occupied by the blue, red, and orange dye was found to be 305, 312, and $308 \text{ m}^2 \text{ g}^{-1}$, respectively (Table 3). These high surface area values indicate a high specific surface area of the Q-CNF aerogel, resulting from the nanoscale width of the constituent cellulose nanofibrils and their formation of a 3D interconnected network structure. The chemical linkage between fibrils helped to freeze this network structure and preserve the high available surface area. The specific surface area A of the cellulose fibrils can be obtained from Eq. (6).

$$A = \frac{m}{\rho_{\text{cellulose}}} \frac{A_{\text{single}}}{V_{\text{single}}}, \quad (6)$$

where $\rho_{\text{cellulose}}$ is the density of cellulose (1.50 g cm^{-3}), while A_{single} and V_{single} represent the surface area and volume of a single nanocellulose fibril, respectively. Assuming a cylindrical shape for the cellulose nanofibril, with diameter D , Eq. (6) yields Eq. (7):

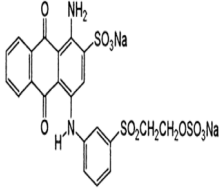
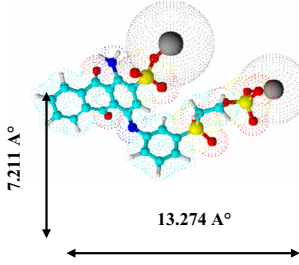
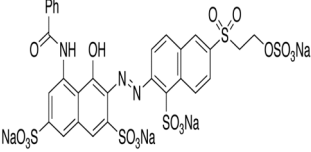
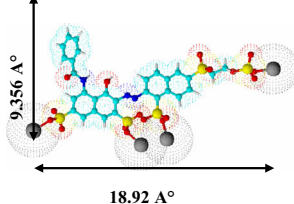
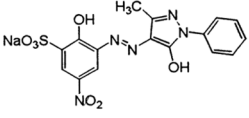
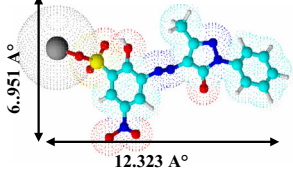
$$A = \frac{m_{\text{nanocellulose}}}{\rho_{\text{cellulose}}} \frac{4}{D}. \quad (7)$$

For a CNF with average diameter of 6 nm, the specific area calculated using Eq. (6) is about $440 \text{ m}^2 \text{ g}^{-1}$. This value is the maximum surface area assuming that all the cellulose nanofibrils have uniform diameter. The lower surface occupied by adsorbed dye molecules could be explained by the possible occurrence of partial aggregation among nanofibrils during lyophilization or a high density of interfibril bonded area, inevitably leading to loss of available surface.

Adsorption mechanism

To further support the adsorption mechanism, zeta potential measurements were carried out on Q-CNF in absence and presence of increasing concentration of dyes (Fig. 8a). Measurements were carried out in presence of Q-CNF gel without crosslinking with isocyanate to preserve the electrophoretic mobility of the cellulose nanofibrils under the effect of the electrical field, so that zeta-potential measurements could be implemented. The Q-CNF exhibited a positive zeta potential, indicating a positively charged surface, resulting from presence of TMA groups on the CNF surface. When dye was added to the CNF suspension, a continuous decrease in the zeta potential was observed as the concentration of the dye was increased, indicating a decrease in the positive surface charge density on the CNFs via charge neutralization between sulfonate groups of dye and TMA groups of CNF. However, the plateau value of the zeta potential differed according to the dye structure, reaching about -10 , 0 , and 3 mV in presence of red, blue, and orange dye, respectively. Although the difference between these values is not large, it indicates that the surface of the dye-saturated CNF bears negative and positive charge in presence of blue and orange dye, respectively, while in presence of red dye, there was total charge compensation and the surface was not charged. This phenomenon is likely due to the difference in the number of sulfonate groups per dye molecule. More specifically, in the case of red dye bearing four sulfonate groups per molecule, total compensation of these negative charges with an equivalent amount of positive charge from TMA on the CNF surface is not possible at saturation, and some of the sulfonate groups remain unbalanced by TMA groups. In the presence of orange dye, the opposite trend will occur, with a fraction of the positive sites on the CNF surface remaining unbalanced by sulfonate groups due to steric restriction. A schematic illustration of the arrangement of dye molecules at saturation is presented in Fig. 8b. The zeta potential analysis further confirmed that adsorption of the dyes by the Q-CNF aerogel was driven by electrostatic attraction between positively charged TMA groups and negative sulfonate groups of the dyes. However, given the planar structure of the dyes used, hydrogen bonding and van der Waals interaction cannot be ignored.

Table 3 Chemical structure and occupied surface of dyes adsorbed on Q-CNF

Chemical formula And abbreviation	Chemical structure drawn with ACD/3D	M (g/mol)	Q _{max} (μmol/g)	Area of dye molecule (Å ²)	Occupied surface area (m ² ·g ⁻¹)	N (SO ₃ ⁻)/ N (NR ₃ ⁺)
 Bleu dye (19)		626.55	531	95.5	302	0.932
 Red dye 180(RD)		933.76	293	176.9	312	1.01
 Orange dye 142(OD)		441.35	600	85.6	308	0.521

The thermodynamic parameters, viz. the free energy of adsorption ΔG° , entropy ΔS° , and enthalpy ΔH° , for the adsorption process by the Q-CNF aerogel were determined using the Van 't Hoff Eq. (6):

$$\ln K_c = \ln \frac{q_e}{C_e} = \frac{\Delta S}{R} - \frac{\Delta H}{RT}, \quad (6)$$

where K_c is the equilibrium distribution coefficient ($K_c = q_e/C_e$), q_e and C_e are the amounts adsorbed at equilibrium and the equilibrium concentration, respectively, R is the gas constant ($8.314 \text{ J mol}^{-1} \text{ K}^{-1}$), and T is temperature (K).

The enthalpy change was obtained by calculating the slope of a plot of $\ln K_c$ versus $1/T$. The thermodynamic results are listed in Table 4. The R^2 values of

the linear fit were at least 0.98, confirming the reliability of the calculated enthalpy and entropy values.

The free energy of adsorption (ΔG°) was negative at all the studied temperatures, reflecting the spontaneity of the process. Positive enthalpy of adsorption was found, implying that the adsorption process is endothermic. The ΔH° values were negative due to the heat released after bond formation between the solute and adsorbent. The values in the range from -50 to -70 kJ mol^{-1} reveal that the adsorption is driven by electrostatic interactions and hydrogen bonding (Faust and Aly 1987). The negative values of ΔS° indicate increased order of the adsorbed dye molecules following immobilization on the CNF surface.

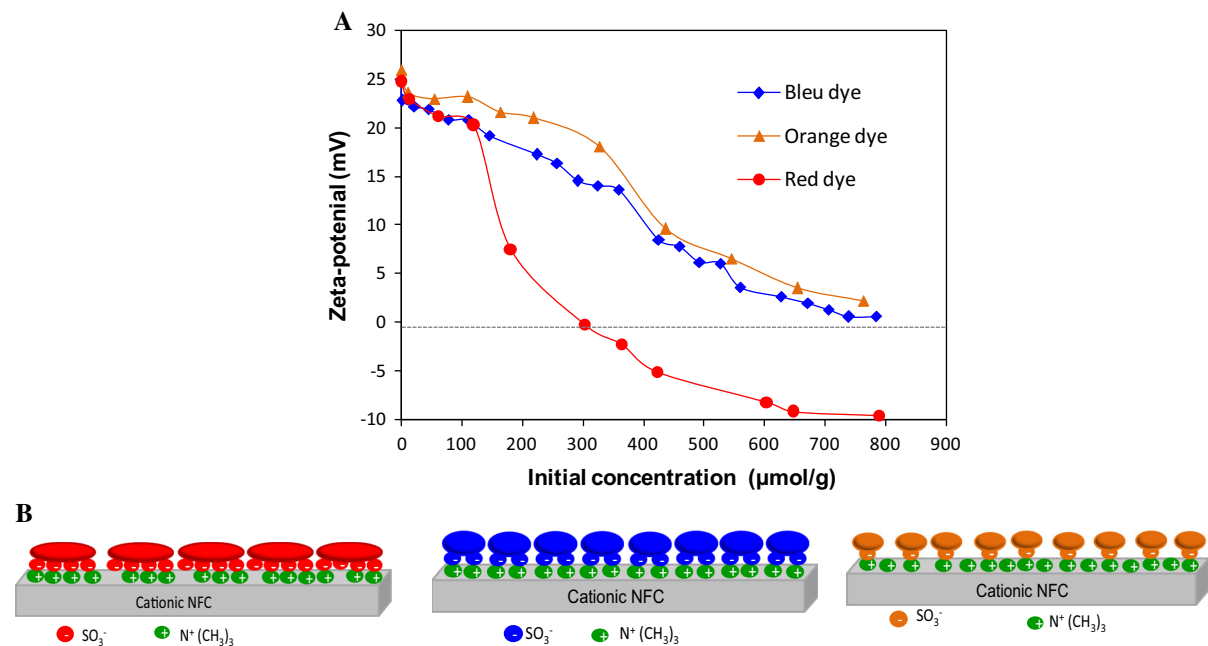


Fig. 8 **a** Change of zeta potential of Q-CNF at pH 7, according to the initial concentration of dye added, after equilibrium during 1 h. **b** Illustration of adsorption of blue, red, and orange dyes on Q-CNF

Table 4 Thermodynamic parameters for adsorption of blue, red, and orange dyes on Q-CNF aerogel

T (K)	ΔG (kJ mol ⁻¹)			ΔH (kJ mol ⁻¹)			ΔS (kJ mol ⁻¹)		
	Blue	Red	Orange	Blue	Red	Orange	Blue	Red	Orange
308	-12.04	-13.064	-18.47	-53.64	-70.38	-51.59	-134.52	-184.23	-109.16
318	-10.813	-12.537	-16.82						
328	-9.271	-9.296	-16.255						

Regeneration and recycling of spent Q-CNF aerogel

Regeneration of the Q-CNF aerogel adsorbent was also studied to investigate its reuse once exhausted. Since the adsorption was mainly driven by electrostatic interactions, the interaction between the adsorbed dye and surface might be weakened by screening the electrostatic interaction with addition of monovalent salt (Bjelopavlic et al. 1999). This approach was shown to be ineffective when an aqueous solution of KCl was used to desorb dyes, even at temperature above 70 °C and salt concentration above 5×10^{-2} M. However, when a solution of KCl in a mixture of water–ethanol (50/50 v/v) was

used, it was possible to remove the adsorbed dye when the treatment was implemented at 70 °C, as shown in Fig. 9. With 10^{-2} M solution of KCl in water–ethanol mixture, more than 95% of the adsorbed dye could be removed in one step, and the regenerated adsorbent was further applied in the next adsorption cycle.

The low release efficiency of adsorbed dye observed for KCl solution in water presumably results from the strong interaction between dye molecules and the CNF surface through multiple binding sites, but also to the decrease in the dye solubility as the ionic strength increases. This latter effect accounts for the increase in the adsorption effectiveness with the ionic strength (Fig. 1SM, supplementary material). For this reason, addition of ethanol to the KCl solution is

necessary to enhance the solubility of the desorbed dye. Recycling of the Q-CNF adsorbent did not affect its adsorption capacity even after more than 20 adsorption–desorption cycles. Note that all the adsorption tests were carried out using the same series of Q-CNF aerogel, which were applied in more than 20 adsorption–desorption cycles, further demonstrating the great potential of this cellulose-based aerogel for practical removal of dyes from water effluent.

Adsorption in continuous-flow fixed-bed column

Traditionally, adsorption isotherms have been used to determine the overall performance of an adsorbent. However, in practice, the commonest and most efficient approach for purification is via column-type operation under continuous flow. To explore the adsorption capacity during such continuous operation, a laboratory glass column filled with Q-CNF aerogel was designed. The column was filled with the pellets of Q-CNF aerogel and percolated from the bottom to the top at linear flow rate of 5 ml min^{-1} using a pressure-adjustable peristaltic pump (Fig. 10). The ratio of the eluted concentration C_s to the input concentration C_0 (i.e., C_s/C_0) was plotted against time to obtain the breakthrough curve at constant flow rate. The breakthrough volume, defined as the point at which the concentration of the eluent reaches 5% of the input concentration, was found to be around 100 ml. The maximum uptake by the column before exhaustion was $262 \mu\text{mol g}^{-1}$, about 50% lower than the adsorption capacity under batch conditions. Work

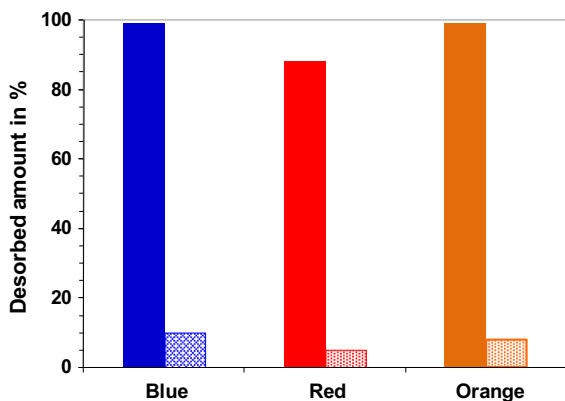


Fig. 9 Desorbed fraction of dyes according to stripping solution: KCl in water (dashed), and KCl in water–ethanol (50/50 vol%) (filled)

is underway to further investigate the effect of operational conditions (flow rate, temperature, bed length, and initial concentration) on the removal efficiency under dynamic conditions.

Resistance to bacterial proliferation

To evaluate the resistance of the aerogel to bacterial growth, the diffusion method was adopted using Gram-positive *Bacillus cereus* (ATCC 14579) and Gram-negative *Escherichia coli* (ATCC 25922). For this test, cationic Q-CNF in thin-film form was used, as well as anionic CNF (A-CNF) for comparison.

Figure 11 shows the results of the diffusion assay for the Q-CNF and A-CNF films. A-CNF could not prevent biofilm formation of *E. coli*, as attested by the proliferation of bacteria growing on the agar plates as well as the surface of the A-CNF films. A-CNFs are cellulose nanofibrils bearing carboxylic groups produced by high-pressure homogenization, obtained from cellulose fibers containing carboxylic groups. On the other hand, for Q-CNF, bacteria proliferated on the agar plates around the films, but not on top or under the films, and no trace of colonization of the film was observed. The Q-CNF aerogel showed significantly improved biofilm inhibition properties and prevented further bacterial growth. This good resistance of Q-CNF to bacterial growth is important for long-term use as an adsorbent, especially for a polysaccharide-based adsorbent, because of the sensitivity of such material to bacterial degradation, inevitably leading to reduction and even loss of adsorption efficiency.

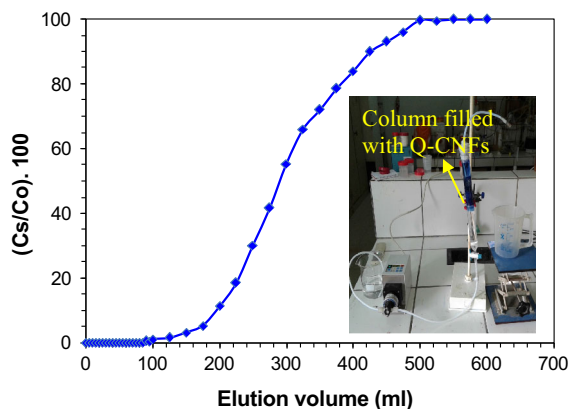


Fig. 10 Breakthrough curve of blue dye for Q-CNF aerogel under continuous flow (Q-CNF aerogel; $C_0 = 5.10^{-4} \text{ M}$; flow rate = 5 ml min^{-1} ; temperature $25 \text{ }^\circ\text{C}$)

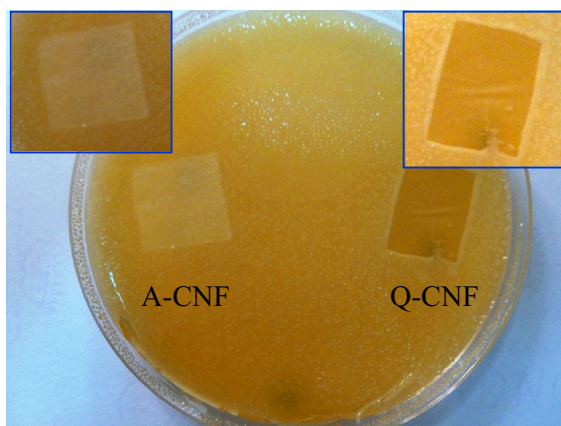


Fig. 11 Petri dishes with NB agar inoculated with *E. coli* in presence of A-CNF and Q-CNF films

The efficient antibacterial activity of Q-NFC against a broad range of bacteria is likely due to the presence of quaternary ammonium groups on the surface of the C-NFC. These groups are known to be one of the most useful antiseptics and disinfectants, being used in a wide range of applications, e.g., in cosmetic products, for clinical purposes, and in textiles and active packaging. The mechanism proposed to account for these strong antibacterial properties is interaction with lipids and proteins composing the cytoplasmic membrane, damaging the outer layer of the bacteria and disturbing their metabolism (Denyer 1995).

Conclusions

A cellulose-based adsorbent in the form of a highly porous aerogel was prepared from cationic CNFs and used as an adsorbent for dye removal. The porous aerogel was prepared by freeze drying a suspension of Q-CNFs (1.5 wt%) to remove water without collapse of the pore structure under the effect of capillary forces. Crosslinking treatment with a trifunctional isocyanate was then carried out to prevent physical disintegration of the hydrophilic cellulose aerogel during immersion in water. Trimethylammonium groups, used to facilitate the CNF production, were found to provide effective binding sites for anionic dyes, resulting in excellent dye removal efficiency from aqueous solution. Zeta potential analysis confirmed the key role of cationic sites on the surface of

the CNFs in controlling the adsorption process through electrostatic interactions between positively charged TMA groups and negative sulfonate groups of dyes. Given the strong interaction between the dye molecules and CNF surface, the dye molecules are expected to lie flat on the surface, favoring occupation of the full available area of the cellulose adsorbent. Spent adsorbent was easily regenerated for reuse in multiple adsorption–desorption cycles by extraction of adsorbed dyes with KCl solution in water–ethanol mixture at 70 °C. Tests conducted in dynamic conditions using a fixed-bed packed column showed the viability of the Q-CNF cross-linked aerogel for such treatments. This result further confirms the great promise of such Q-CNF solid aerogels as a new class of functional nanosized bioadsorbents for dye removal from wastewater. Work is in progress to generate both anionic and cationic sites on the surface of CNFs to produce a dual adsorbent for removal of both anionic and cationic dyes.

References

- Abdul Khalil HPS, Davoudpour Y, Islama MdN, Mustapha A, Sudeshd K, Dunganian R, Jawaid M (2014) Production and modification of nanofibrillated cellulose using various mechanical processes. *Carbohydr Polym* 99:649–665
- Alcalá M, González I, Boufi S, Vilaseca F, Mutjé P (2013) All-cellulose composites from unbleached hardwood kraft pulp reinforced with nanofibrillated cellulose. *Cellulose* 20:2909–2921
- Bjelopavlic M, Newcombe G, Hayes R (1999) Adsorption of NOM onto activated carbon: effect of surface charge, ionic strength, and pore volume distribution. *J Colloid Interface Sci* 210:271–282
- Boufi S (2014) Chapter 14. In: Hakeem KR, Jawaid M, Rashid U (eds) *Biomass and bioenergy*. Springer, Berlin, pp 267–305
- Boufi S, Kaddami H, Dufresne A (2014) Mechanical performance and transparency of nanocellulose reinforced polymer nanocomposites. *Macromol. Mater. Eng.* 299:560–568
- Chaker A, Boufi S (2015) Cationic nanofibrillar cellulose with high antibacterial properties. *Carbohydr Polym* 131:224–232
- Denyer SP (1995) Mechanisms of action of antibacterial biocides. *Int Biodeterior Biodegradation* 36:227–245
- Dufresne A (2013) Nanocellulose: a new ageless bionanomaterial. *Mater Today* 16:220–226
- Eyley S, Thielemans W (2014) Surface modification of cellulose nanocrystals. *Nanoscale*. 6:7764–7773
- Faust S, Aly O (1987) *Adsorption processes for water treatment*. Butterworth, Oxford

- García-González CA, Alnaief M, Smirnova I (2011) Polysaccharide-based aerogels—Promising biodegradable carriers for drug delivery systems. *Carbohydr Polym* 86:1425–1438
- González I, Boufi S, Pèlach MA, Alcalá M, Vilaseca F, Mutjé P (2012) Nanofibrillated cellulose as paper additive in eucalyptus pulps. *BioResources*. 4:5167–5180
- González I, Vilaseca F, Alcalá M, Pèlach MA, Boufi S, Mutjé P (2013) Effect of the combination of biobeating and CNF on the physico-mechanical properties of paper. *Cellulose* 20:1425–1435
- Hall KR, Eagleton LC, Acrivos A, Vermeulen T (1966) *Ind Eng Chem Fundam* 5:212
- Ho TTT, Zimmermann T, Hauert R, Caseri W (2011) Preparation and characterization of cationic nanofibrillated cellulose from etherification and high-shear disintegration processes. *Cellulose* 18:1391–1406
- Kalia S, Boufi S, Celli A, Kango S (2014) Nanofibrillated cellulose: surface modification and potential applications. *Colloid Polym Sci* 292:5–31
- Kim CH, Youn HJ, Lee HL (2015) Preparation of cross-linked cellulose nanofibril aerogel with water absorbency and shape recovery. *Cellulose* 22:3715–3724
- Maatar W, Boufi S (2015) Poly (methacrylic acid-co-maleic acid) grafted nanofibrillated cellulose as a reusable novel heavy metal ions adsorbent. *Carbohydr Polym* 126:199–207
- Mathew AP, Oksman K, Pierron D, Harmand MF (2012) Fibrous cellulose nanocomposite scaffolds prepared by partial dissolution for potential use as ligament or tendon substitutes. *Carbohydr Polym* 87:2291–2298
- Olszewska A, Eronen P, Johansson LS, Malho JM, Ankerfors M, Lindstrom T, Ruokolainen J, Laine J, Osterberg M (2011) The behaviour of cationic NanoFibrillar Cellulose in aqueous media. *Cellulose* 18:1213–1226
- Pei A, Butchosa N, Berglund LA, Zhou Q (2013) Surface quaternized cellulose nanofibrils with high water absorbency and adsorption capacity for anionic dyes. *Soft Matter* 9:2047–2055
- Ray MS (1996) Adsorption and adsorptive separations. *Adsorption* 2:157–178
- Richard M (1996) Principles of Adsorption and Reaction on Solid Surfaces. Wiley Interscience, New York
- Saini S, Falco CY, Belgacem MN, Bras J (2016) Surface cationized cellulose nanofibrils for the production of contact active antimicrobial surfaces. *Carbohydrate Polym*. 135:239–247
- Tanpichai S, Quero F, Nogi M, Yano H, Young RJ, Lindström T, Sampson WW, Eichhorn SJ (2012) Effective Young's modulus of bacterial and microfibrillated cellulose fibrils in fibrous networks. *Biomacromolecules* 13:1340–1349
- Yang X, Al-Duri B (2005) Kinetic modeling of liquid-phase adsorption of reactive dyes on activated carbon. *J Colloid Interface Sci* 287:25–34
- Zhang W, Zhang Y, Lu C, Deng Y (2012) Aerogels from crosslinked cellulose nano/micro-fibrils and their fast shape recovery property in water. *J Mater Chem* 22:11642